

## Alzheimer Hastalığı için Potansiyel Çok Hedefli Terapötikler Olarak Stilbenlerin Hesaplamalı Analizi

Seda ŞİRİN<sup>1\*</sup>

<sup>1</sup>Gazi Üniversitesi, Fen Fakültesi, Biyoloji Bölümü, 06500, Teknikokullar, Ankara, Türkiye

<sup>1</sup><https://orcid.org/0000-0003-2636-725X>

\*Sorumlu yazar: [sdasirin@hotmail.com](mailto:sdasirin@hotmail.com)

### Araştırma Makalesi

#### Makale Tarihi:

Geliş tarihi: 08.04.2024

Kabul tarihi: 21.08.2024

Online Yayınlanma: 15.01.2025

#### Anahtar Kelimeler:

Alzheimer hastalığı

FDA onaylı ilaçlar

Moleküler yerleştirme

Stilben

SWISS ADME

### ÖZ

Bu çalışmanın amacı, 13 stilben ve Alzheimer hastalığı (AH)'nın tedavisinde kullanılan 5 Amerikan Gıda ve İlaç Dairesi onaylı ilacın ADME tahmini ve moleküler yerleştirme yöntemi ile karşılaştırılmasıdır. AH patolojisinde yer alan kolinerjik, amiloid, tau, oksidatif stres ve inflamasyon hipotezleri, moleküler yerleştirmede hedeflenmiştir. SwissADME, stilbenlerin (resveratrol, pterostilben, oksiresveratrol, piceatannol, pinosilvin, isorhapontigenin, isorhapontin, astringin, piceid (polidatin) ve mulberroside A) ve Amerikan Gıda ve İlaç Dairesi onaylı ilaçların (takrin, donepezil, rivastigmin, galantamin ve memantin) fizikokimyasal, lipofiliklik, suda çözünürlük, farmakokinetik, ilaca benzerlik ve tıbbi kimya özelliklerini belirlemek için kullanılmıştır. CBDOCK2, stilbenlerin ve Amerikan Gıda ve İlaç Dairesi onaylı ilaçların hedef proteinlere (AChE, BuChE, APP, BACE, GSK-3 $\beta$ , CDK5, SOD, CAT, GPx, Cox-2, iNOS, IL-1 $\beta$  ve TNF- $\alpha$ ) bağlanma afinitesini belirlemek için kullanılmıştır. SwissADME sonuçları stilbenlerin AH tedavisinde doğal ürünler olarak kullanılabileceğini göstermiştir. Moleküler yerleştirme sonuçları, mulberroside A'nın en iyi vına skorunu (kcal/mol) gösterdiğini ve ardından astringin, piceid (polidatin), isorhapontin, donepezil, oxyresveratrol, piceatannol, galantamin, resveratrol, isorhapontigenin, takrin, pinosilvin, pterostilben, rivastigmin ve memantin'in geldiği gösterilmiştir. Çalışmamızda AH tedavisinde stilbenler ve Amerikan Gıda ve İlaç Dairesi onaylı ilaçlar hesaplamalı yaklaşımlar kullanılarak değerlendirilmiştir. Sonuçlar, AH patolojisinin çeşitli hipotezleri üzerindeki potansiyel terapötik etkilerini vurgulamıştır. Bu bulguların klinik uygulamalarda doğrulanması için daha fazla araştırmaya ihtiyaç vardır.

## Computational Analysis of Stilbenes as Potential Multi-Targeted Therapeutics for Alzheimer's Disease

### Research Article

#### Article History:

Received: 08.04.2024

Accepted: 21.08.2024

Published online: 15.01.2025

#### Keywords:

Alzheimer's disease

FDA-approved drugs

Molecular docking

Stilbene

SWISS ADME

### ABSTRACT

The aim of this study is to compare 13 stilbenes and 5 FDA-approved drugs used in the treatment of Alzheimer's disease (AD) by ADME prediction and molecular docking method. Cholinergic, amyloid, tau, oxidative stress and inflammation hypotheses involved in AD pathology were targeted in molecular docking. SwissADME has been used to determine the physicochemical, lipophilicity, water solubility, pharmacokinetics, drug-likeness and medicinal chemistry properties of stilbenes (resveratrol, pterostilbene, oxyresveratrol, piceatannol, pinosylvin, isorhapontigenin, isorhapontin, astringin, piceid (polydatin), and mulberroside A) and FDA-approved drugs (tacrine, donepezil, rivastigmine, galantamine, and memantine). CBDOCK2 has been used to determine the binding affinity stilbenes and FDA-approved drugs to target proteins (AChE, BuChE, APP,

BACE, GSK-3 $\beta$ , CDK5, SOD, CAT, GPx, Cox-2, iNOS, IL-1 $\beta$ , and TNF- $\alpha$ ). SwissADME results showed that stilbenes could be used as natural products in the treatment of AD. The molecular docking results indicated that mulberroside A showed the best vina score (kcal/mol) followed by astringin, piceid (polydatin), isorhapontin, donepezil, oxyresveratrol, piceatannol, galanthamine, resveratrol, isorhapontigenin, tacrine, pinosylvin, pterostilbene, rivastigmine, and memantine. Our study evaluated stilbenes and FDA-approved drugs for the treatment of AD using computational approaches. The results highlight its potential therapeutic effects on various hypotheses of AD pathology. More research is needed to validate these findings for clinical practice.

---

**To Cite:** Şirin S. Computational Analysis of Stilbenes as Potential Multi-Targeted Therapeutics for Alzheimer's Disease. *Osmaniye Korkut Ata Üniversitesi Fen Bilimleri Enstitüsü Dergisi* 2025; 8(1): 145-166.

## 1. Introduction

Alzheimer's disease (AD) is a severe neurological disorder that results in dementia and is thought to be responsible for 60% to 70% of cases worldwide. Patients sixty to sixty-five years of age and older are affected by AD, a degenerative disorder. In this age range, it is the primary cause of death. Epidemiological projections suggest that by 2050, the number of people with AD globally may rise to 107 million in rising economies (Kamble et al., 2024).

The development of AD is thought to be influenced by several theories, including cholinergic, amyloid, tau, oxidative stress, and inflammatory ones (Shevelyova et al., 2024). The cholinergic theory states that increased acetylcholine esterase (AChE) breakdown of acetylcholine (ACh) into acetate and choline causes ACh levels to decrease in AD. Lower levels of ACh affect brain activity and encourage the aggregation of amyloid-beta (A $\beta$ ), which results in the formation of senile plaque (Vejandla et al., 2024). The amyloid theory postulates that the accumulation of A $\beta$ , (amyloid precursor protein (APP) which is processed by proteases to produce A $\beta$ ) sets off a series of processes that eventually result in neurodegeneration (Ganz and Ben-Hur, 2024; Wolfe, 2024). According to the Tau theory, AD is primarily caused by an accumulation of abnormal Tau protein in the brain (Liu et al., 2024; Nasb et al., 2024). Reactive oxygen species (ROS) cause damage to brain cells under oxidative stress, which leads to neurodegeneration and cognitive decline, according to the oxidative stress and inflammation theories. Both A $\beta$  and phosphorylated tau pathologies lead to enhanced ROS generation. ROS can cause an inflammatory response, whereas inflammation causes oxidative stress. Oxidative stress and inflammation can damage synapses and brain cells, contributing to A $\beta$  and tau neurotoxicity in AD (Perluigi et al., 2024).

Because AD is so complicated, FDA-approved drugs (tacrine, donepezil, rivastigmine, galantamine, and memantine) that interacts with a single receptor or enzyme is frequently insufficient for therapy (Yajing et al., 2024). Because there are so few viable therapy options for AD, researchers are looking into powerful pharmacological drugs as well as a wide range of other biological processes as ways to prevent it. As a result, dietary small molecules from natural sources were studied and shown to have potential therapeutic effects in AD. These compounds (e.g., flavonoid polyphenols, phenolic acids, stilbenes, and

lignans) have been widely documented to be anti-AD agents both *in vivo* and *in vitro*, with relatively modest side effects (Balakrishnan et al., 2024).

Polyphenols are categorized into four kinds based on their structural properties and number of phenolic rings: flavonoid polyphenols, phenolic acids, stilbenes, and lignans. Stilbenes are important phytoestrogens, referring to a family of polyphenolic compounds having a homogenous stilbene parent nucleus or its polymers (Cao et al., 2024). These compounds are made up of two benzene rings arranged C6-C2-C6. Many stilbenes are generated from trans-resveratrol or t-resveratrol, which is an essential precursor in their synthesis. T-resveratrol can be transformed into various stilbenes, including viniferins (by oxidation), pterostilbene (via methylation), and piceid (via glycosylation) (Aleynova et al., 2024). Stilbenes, due to their unique molecular structure, have been shown to exhibit a variety of pharmacological properties, including antioxidant, anti-inflammatory, and anti-degenerative disease effects (Socala et al., 2024; Yan et al., 2024).

The current study aims to evaluate the stilbenes (resveratrol, pterostilbene, oxyresveratrol, piceatannol, pinosylvin, isorhapontigenin, isorhapontin, astringin, piceid (polydatin), and mulberroside A), compared to the FDA-approved drugs (tacrine, donepezil, rivastigmine, galantamine, and memantine), to treat AD by targeting the cholinergic hypothesis (AChE and BuChE), the amyloid hypothesis (APP and BACE), the tau hypothesis (GSK-3 $\beta$  and CDK5), the hypotheses of oxidative stress (SOD, CAT, and GPx) and inflammation (Cox-2, iNOS, IL-1 $\beta$ , and TNF- $\alpha$ ) by computational approaches through, ADME (absorption, distribution, metabolism, and excretion) prediction and molecular docking.

## 2. Material and Methods

### 2.1. Preparation of ligands, FDA-approved drugs, and proteins

Ligands (resveratrol, pterostilbene, oxyresveratrol, piceatannol, pinosylvin, isorhapontigenin, isorhapontin, astringin, piceid (polydatin), and mulberroside A) and FDA-approved drugs (tacrine, donepezil, rivastigmine, galantamine, and memantine) for SwissADME online platform were prepared in SMILES string format (Table 1).

**Table 1.** Stilbenes and FDA-approved drugs list

Ligand Name	SMILES String
Resveratrol (1)	<chem>Oc2ccc(C=Cc1cc(O)cc(O)c1)cc2</chem>
Pterostilbene (2)	<chem>COc2cc(OC)cc(C=Cc1ccc(O)cc1)c2</chem>
Oxyresveratrol (3)	<chem>Oc2ccc(C=Cc1cc(O)cc(O)c1)c(O)c2</chem>
Piceatannol (4)	<chem>Oc2cc(O)cc(C=Cc1ccc(O)c(O)c1)c2</chem>
Pinosylvin (5)	<chem>Oc2cc(O)cc(C=Cc1ccccc1)c2</chem>
Isorhapontigenin (6)	<chem>COc2cc(C=Cc1cc(O)cc(O)c1)ccc2O</chem>
Isorhapontin (7)	<chem>COc3cc(C=Cc2cc(O)cc(OC1OC(CO)C(O)C(O)C1O)c2)ccc3O</chem>
Astringin (8)	<chem>OCC3OC(Oc2cc(O)cc(C=Cc1ccc(O)c(O)c1)c2)C(O)C(O)C3O</chem>
Piceid (polydatin) (9)	<chem>OCC3OC(Oc2cc(O)cc(C=Cc1ccc(O)cc1)c2)C(O)C(O)C3O</chem>
Mulberroside A (10)	<chem>OCC4OC(Oc3ccc(C=Cc2cc(O)cc(OC1OC(CO)C(O)C(O)C1O)c2)c(O)c3)C(O)C(O)C4O</chem>
Tacrine (11)	<chem>Nc2c1CCCCc1nc3ccccc23</chem>
Donepezil (12)	<chem>COc4cc3CC(CC1CCN(CC1)Cc2ccccc2)C(=O)c3cc4OC</chem>
Rivastigmine (13)	<chem>CCN(C)C(=O)Oc1cccc(c1)C(C)N(C)C</chem>
Galantamine (14)	<chem>COc2ccc3CN(C)CCC14C=CC(O)CC1Oc2c34</chem>
Memantine (15)	<chem>CC13CC2CC(C)(C1)CC(N)(C2)C3</chem>

Also, ligands (resveratrol, pterostilbene, oxyresveratrol, piceatannol, pinosylvin, isorhapontigenin, isorhapontin, astringin, piceid (polydatin), and mulberroside A), FDA-approved drugs (tacrine, donepezil, rivastigmine, galantamine, and memantine), and proteins (AChE, BuChE, APP, BACE, GSK-3 $\beta$ , CDK5, SOD, CAT, GPx, Cox-2, iNOS, IL-1 $\beta$ , and TNF- $\alpha$ ) for cavity-detection guided blind docking (CB-DOCK) were prepared in mol2, mol, sdf, and pdb format.

### *2.2. SwissADME online platform*

The ADME prediction server used is SwissADME (<http://swissadme.ch/>) from the Swiss Institute of Bioinformatics. SwissADME has been used to determine the physicochemical properties (formula, molecular weight, num. heavy atoms, num. arom. heavy atoms, fraction Csp3, num. rotatable bonds, num. H-bond acceptors, num. H-bond donors, molar refractivity, and TPSA), lipophilicity (log Po/w (iLOGP, XLOGP3, WLOGP, MLOGP, and SILICOS-IT), and consensus log Po/w), water solubility (log S (ESOL), log S (Ali), log S (SILICOS-IT), solubility (mg/ml; mol/l), and class), pharmacokinetics (GI absorption, BBB permeant, P-gp substrate, CYP1A2, CYP2C19, CYP2C9, CYP2D6, CYP3A4 inhibitor, and Log Kp (skin permeation)), drug-likeness (lipinski, ghose, veber, egan, muegge, and bioavailability score), and medicinal chemistry (PAINS, brenk, leadlikeness, and synthetic accessibility) associated with small molecules (Daina et al., 2017).

### *2.3. CB-DOCK2 online platform*

The protein-ligand blind docking server used is CB-DOCK2 (<https://cadd.labshare.cn/cb-dock2/index.php>) from the Cao Lab. CB-DOCK2 has been used to determine the protein-ligand blind docking, integrating cavity detection, docking and homologous template fitting (Liu et al., 2022).

## **3. Results and Discussion**

Comprehensive evaluation of stilbenes such as resveratrol, pterostilbene, oxyresveratrol, piceatannol, pinosylvin, isorhapontigenin, isorhapontin, astringin, piceid (polydatin), and mulberroside A, as well as FDA-approved drugs, including tacrine, donepezil, rivastigmine, galantamine, and memantine, have shown their potential for AD. It constitutes an important step in the evaluation of treatments. Through computational methodologies involving ADME prediction and molecular docking, this study investigates multifaceted aspects of AD pathology, specifically targeting cholinergic, amyloid, and tau hypotheses, as well as oxidative stress and inflammation. In the following section, we will describe the findings of our research, shedding light on the effectiveness and potential mechanisms of action of these stilbenes and FDA-approved drugs in combating the progression of AD.

### 3.1. Bioavailability radar of the ligands and FDA-approved drugs

The bioavailability radar of the ligands (resveratrol, pterostilbene, oxyresveratrol, piceatannol, pinosylvin, isorhapontigenin, isorhapontin, astringin, piceid (polydatin), and mulberroside A) and FDA-approved drugs (tacrine, donepezil, rivastigmine, galantamine, and memantine) are shown in Figure 1. Bioavailability radar provides a first look at the drug-likeness of ligands and FDA-approved drugs. This radar is used to determine the potential of molecules as drugs by evaluating their pharmacokinetic and pharmacodynamic properties (Jia et al., 2020; Ranjith and Ravikumar, 2019). This methodology helps identify compounds with drug-like properties and examines critical properties of molecules such as lipophilicity, size, polarity, solubility, saturation, and flexibility (Ibrahim et al., 2020). These evaluation criteria are used to determine the bioavailability of compounds and their potential in the drug development process. Bioavailability radars of FDA-approved drugs with stilbenes are an important tool to determine the pharmacokinetic profiles and drug-likeness of these compounds (Poltronieri et al., 2020). These comprehensive evaluations contribute to the development of more effective treatment strategies. The pink area represents the optimal range for 6 properties (lipophilicity, size, polarity, solubility, saturation, and flexibility) (lipophilicity: XLOGP3 between -0.7 and +5.0, size: MW between 150 and 500 g/mol, polarity: TPSA between 20 and 130 Å<sup>2</sup>, solubility: log S not higher than 6, saturation: carbon fraction in sp<sup>3</sup> hybridization should not be less than 0.25, and flexibility: not more than 9 rotatable bonds) (Ibrahim et al., 2020). Ligands (isorhapontigenin, astringin, piceid (polydatin), and mulberroside A) and FDA-approved drugs (donepezil, rivastigmine, galantamine, and memantine) are within the optimal range for the 6 properties (lipophilicity, size, polarity, solubility, saturation, and flexibility).

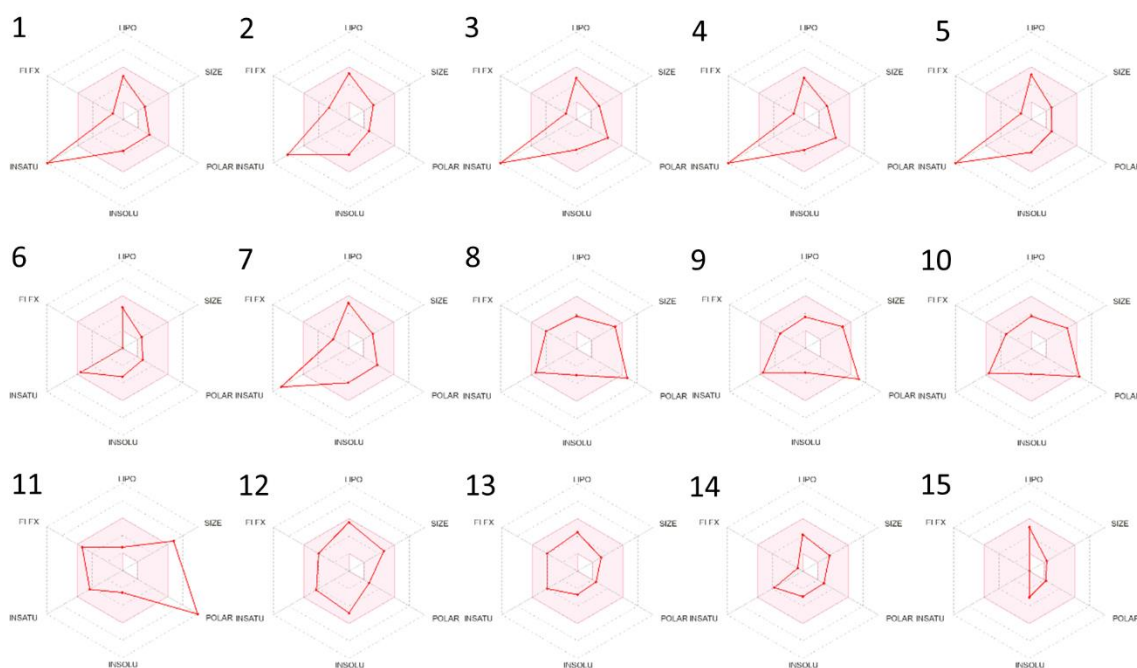


**Figure 1.** Bioavailability radar of ligands and FDA-approved drugs

### 3.2. BOILED-Egg plot of the ligands and FDA-approved drugs

The Brain Or IntestinaL EstimateD permeation method (BOILED-Egg) plot of the ligands (resveratrol, pterostilbene, oxyresveratrol, piceatannol, pinosylvin, isorhapontigenin, isorhapontin, astringin, piceid (polydatin), and mulberroside A) and FDA-approved drugs (tacrine, donepezil, rivastigmine, galantamine, and memantine) are shown in Figure 2.

BOILED-Egg plot estimates passive (P-gp substrate-, red)/active (P-gp substrate+, blue) blood-brain barrier (BBB) permeation and human gastrointestinal absorption (HIA) of ligands and FDA-approved drugs (Ndombera et al., 2019). This prediction is based on 2 physicochemical properties: lipophilicity (WLOGP) and polarity (TPSA) (Daina and Zoete, 2016). The yolk contains the physicochemical domain for BBB permeation and the egg white contains the physicochemical domain for HIA (Rafeeq et al., 2024). The outer gray area represents ligands with properties that imply limited BBB permeation and low HIA (Ponzoni et al., 2017). This model is a critical tool for predicting the bioavailability and efficacy of drugs and evaluates the pharmacokinetic profiles of ligands and drugs. These evaluations contribute to the development of more effective treatment strategies. Ligands [resveratrol (passive), pterostilbene (passive), pinosylvin (passive), and isorhapontigenin (passive), and FDA-approved drugs [tacrine (active), donepezil (active), rivastigmine (passive), galantamine (active), and memantine (passive)] shows high BBB permeation and high HIA.

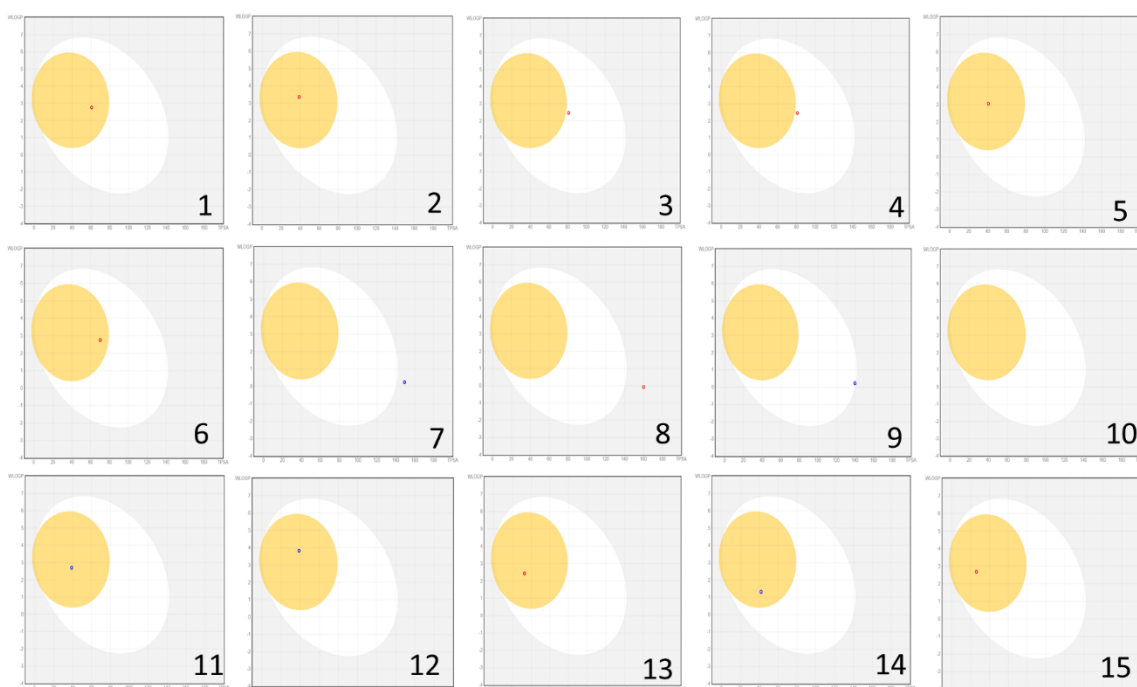


**Figure 2.** BOILED-Egg plot of ligands and FDA-approved drugs

### 3.3. Physicochemical properties of the ligands and FDA-approved drugs

The physicochemical properties of the ligands (resveratrol, pterostilbene, oxyresveratrol, piceatannol, pinosylvin, isorhapontigenin, isorhapontin, astringin, piceid (polydatin), and mulberroside A) and FDA-approved drugs (tacrine, donepezil, rivastigmine, galantamine, and memantine) are shown in Table 2. Physicochemical properties evaluated to understand the pharmacokinetic and pharmacodynamic properties of ligands provide important information about the bioavailability, efficacy and safety of the drug. While the molecular weight (MW) and the number of heavy atoms determine the size and complexity of the compound, the Csp3 fraction affects the three-dimensional structure and bioavailability of the molecule (Rafeeq et al., 2024). The number of rotatable bonds affects the flexibility of the molecule, and the number of hydrogen bond acceptors and donors affects its solubility in aqueous environments and interaction with biological targets (Daina and Zoete, 2016). The bioavailability radar also provides information on the molecular weight (size), fraction csp3 (saturation), number of rotatable bonds (flexibility), and TPSA (polarity) of ligands and FDA-approved drugs (size: MW between 150 and 500 g/mol, saturation: carbon fraction in sp3 hybridization should not be less than 0.25, flexibility: not more than 9 rotatable bonds, and polarity: TPSA between 20 and 130 Å<sup>2</sup>) (Kadri and Aouadi, 2020). All ligands and FDA-approved drugs, except mulberroside A, are within the optimum range for molecular weight (size). All ligands and FDA-approved drugs, except resveratrol, pterostilbene, oxyresveratrol, piceatannol, pinosylvin, and isorhapontigenin, are within the optimum range for fraction csp3 (saturation). All ligands and FDA-approved drugs are within the optimum range for number of rotatable bonds (flexibility). All ligands and FDA-approved drugs, except isorhapontin, astringin, piceid (polydatin), and mulberroside A, are within the optimum range for TPSA (polarity).

**Table 2.** Physicochemical properties of ligands and FDA-approved drugs

Physicochemical Properties										
No	Formula	Molecular weight	Num. heavy atoms	Num. arom. heavy atoms	Fraction Csp3	Num. rotatable bonds	Num. H-bond acceptors	Num. H-bond donors	Molar refractivity	TPSA
1	C14H12O3	228.24 g/mol	17	12	0.00	2	3	3	67.88	60.69 Å <sup>2</sup>
2	C16H16O3	256.30 g/mol	19	12	0.12	4	3	1	76.82	38.69 Å <sup>2</sup>
3	C14H12O4	244.24 g/mol	18	12	0.00	2	4	4	69.90	80.92 Å <sup>2</sup>
4	C14H12O4	244.24 g/mol	18	12	0.00	2	4	4	69.90	80.92 Å <sup>2</sup>
5	C14H12O2	212.24 g/mol	16	12	0.00	2	2	2	65.86	40.46 Å <sup>2</sup>
6	C15H14O4	258.27 g/mol	19	12	0.07	3	4	3	74.37	69.92 Å <sup>2</sup>
7	C21H24O9	420.41 g/mol	30	12	0.33	6	9	6	106.50	149.07 Å <sup>2</sup>
8	C20H22O9	406.38 g/mol	29	12	0.30	5	9	7	102.03	160.07 Å <sup>2</sup>
9	C20H22O8	390.38 g/mol	28	12	0.30	5	8	6	100.00	139.84 Å <sup>2</sup>
10	C26H32O14	568.52 g/mol	40	12	0.46	8	14	10	134.15	239.22 Å <sup>2</sup>
11	C13H14N2	198.26 g/mol	15	10	0.31	0	1	1	63.58	38.91 Å <sup>2</sup>
12	C24H29NO3	379.49 g/mol	28	12	0.46	6	4	0	115.31	38.77 Å <sup>2</sup>
13	C14H22N2O2	250.34 g/mol	18	6	0.50	6	3	0	73.12	32.78 Å <sup>2</sup>
14	C17H21NO3	287.35 g/mol	21	6	0.53	1	4	1	84.05	41.93 Å <sup>2</sup>
15	C12H21N	179.30 g/mol	13	0	1.00	0	1	1	55.68	26.02 Å <sup>2</sup>

### 3.4. Lipophilicity of the ligands and FDA-approved drugs

The lipophilicity of the ligands (resveratrol, pterostilbene, oxyresveratrol, piceatannol, pinosylvin, isorhapontigenin, isorhapontin, astringin, piceid (polydatin), and mulberroside A) and FDA-approved drugs (tacrine, donepezil, rivastigmine, galantamine, and memantine) are shown in Table 3.

The classic descriptor for lipophilicity is the partition coefficient ( $\log P_{o/w}$ ) between N-octanol and water (Buchwald and Bodor, 1998).  $\log P_{o/w}$  was calculated with five different prediction models (iLOGP, XLOGP3, WLOGP, MLOGP and SILICOS-IT) (Mishra and Dahima, 2019). The consensus  $\log P_{o/w}$  is the arithmetic mean of the values estimated by five different prediction models (Udugade et al., 2019).  $\log P_{o/w}$  is ranged between  $-0.7$  and  $+5.0$  according to the bioavailability radar (Sert et al., 2021). This parameter is an important indicator that affects the bioavailability of molecules and their ability to reach target cells. All ligands and FDA-approved drugs, except mulberroside A, are within the optimum range.

**Table 3.** Lipophilicity of ligands and FDA-approved drugs

Lipophilicity						
No	Log Po/w (iLOGP)	Log Po/w (XLOGP3)	Log Po/w (WLOGP)	Log Po/w (MLOGP)	Log Po/w (SILICOS-IT)	Consensus Log Po/w
1	1.71	3.13	2.76	2.26	2.57	2.48
2	3.02	3.78	3.36	2.76	3.61	3.31
3	1.44	2.77	2.46	1.67	2.08	2.08
4	1.61	2.86	2.46	1.67	2.08	2.14
5	2.05	3.48	3.05	2.87	3.07	2.90
6	2.27	3.59	2.76	1.93	2.60	2.63
7	2.25	1.06	0.24	-0.65	0.55	0.69
8	1.27	0.73	-0.07	-0.87	0.00	0.21
9	1.75	1.03	0.23	-0.36	0.47	0.62
10	1.00	-0.84	-2.59	-2.97	-2.08	-1.50
11	2.09	2.71	2.70	2.33	3.12	2.59
12	3.92	4.28	3.83	3.06	4.91	4.00
13	3.21	2.29	2.44	2.34	1.46	2.34
14	2.64	1.84	1.32	1.74	2.03	1.91
15	2.51	3.28	2.69	3.02	2.76	2.85

### 3.5. Water solubility of the ligands and FDA-approved drugs

The water solubility of the ligands (resveratrol, pterostilbene, oxyresveratrol, piceatannol, pinosylvin, isorhapontigenin, isorhapontin, astringin, piceid (polydatin), and mulberroside A) and FDA-approved drugs (tacrine, donepezil, rivastigmine, galantamine, and memantine) are shown in Table 4.

Water solubility ( $\log S$ ) was calculated with three different prediction models (ESOL, Ali, and SILICOS-IT) (Ciorsac et al., 2021). These prediction models play a critical role in evaluating the aqueous solubility of compounds and provide important information in drug discovery and development processes. ESOL, Ali and SILICOS-IT models are used to optimize the bioavailability and efficacy of drugs by determining the solubility profiles of compounds (Boobier et al., 2020). These models provide important tools for understanding and improving the pharmacokinetic and pharmacodynamic properties of drugs.  $\log S$  is ranged between insoluble  $< -10$   $<$  poorly  $< -6$   $<$  moderately  $< -4$   $<$  soluble  $< -2$  very soluble  $< 0$  highly (Yağlıoğlu et al., 2022; Henning et al., 2023). All ligands and FDA-approved drugs are within the optimum range for soluble, moderately soluble, and poorly soluble classes.



**Table 4.** Water solubility of ligands and FDA-approved drugs

Water solubility									
No	Log S (ESOL)	Solubility (mg/ml;mol/l)	Class	Log S (Ali)	Solubility (mg/ml;mol/l)	Class	Log S (SILICOS-IT)	Solubility (mg/ml;mol/l)	Class
1	3.62	5.51e-02; 2.41e-04	Soluble	-4.07	1.93e-02; 8.44e-05	Moderately soluble	-3.29	1.18e-01; 5.16e-04	Soluble
2	-4.01	2.48e-02; 9.69e-05	Moderately soluble	-4.29	1.33e-02; 5.17e-05	Moderately soluble	-4.69	5.24e-03; 2.05e-05	Moderately soluble
3	-3.46	8.45e-02; 3.46e-04	Soluble	-4.12	1.83e-02; 7.50e-05	Moderately soluble	-2.71	4.75e-01; 1.95e-03	Soluble
4	-3.52	7.42e-02; 3.04e-04	Soluble	-4.22	1.48e-02; 6.05e-05	Moderately soluble	-2.71	4.75e-01; 1.95e-03	Soluble
5	-3.77	3.59e-02; 1.69e-04	Soluble	-4.01	2.06e-02; 9.73e-05	Moderately soluble	-3.86	2.92e-02 ; 1.38e-04	Soluble
6	-3.97	2.75e-02; 1.07e-04	Soluble	-4.74	4.65e-03; 1.80e-05	Moderately soluble	-3.41	1.00e-01; 3.88e-04	Soluble
7	-3.01	4.07e-01; 9.68e-04	Soluble	-3.78	6.95e-02; 1.65e-04	Soluble	-1.71	8.24e+00; 1.96e-02	Soluble
8	-2.80	6.51e-01; 1.60e-03	Soluble	-3.67	8.68e-02; 2.14e-04	Soluble	-1.02	3.90e+01; 9.59e-02	Soluble
9	-2.90	4.96e-01; 1.27e-03	Soluble	-3.56	1.08e-01; 2.78e-04	Soluble	-1.61	9.67e+00; 2.48e-02	Soluble
10	-2.53	1.68e+00; 2.95e-03	Soluble	-3.70	1.13e-01; 1.98e-04	Soluble	0.76	3.29e+03; 5.79e+00	Soluble
11	-3.27	1.07e-01; 5.37e-04	Soluble	-3.18	1.31e-01; 6.60e-04	Soluble	-4.46	6.95e-03; 3.51e-05	Moderately soluble
12	-4.81	5.87e-03; 1.55e-05	Moderately soluble	-4.81	5.92e-03; 1.56e-05	Moderately soluble	-6.90	4.78e-05; 1.26e-07	Poorly soluble
13	-2.69	5.17e-01; 2.06e-03	Soluble	-2.62	6.06e-01; 2.42e-03	Soluble	-3.15	1.76e-01; 7.01e-04	Soluble
14	-2.93	3.41e-01; 1.19e-03	Soluble	-2.34	1.31e+00; 4.56e-03	Soluble	-2.96	3.17e-01; 1.10e-03	Soluble
15	-3.02	1.72e-01; 9.59e-04	Soluble	-3.50	5.65e-02; 3.15e-04	Soluble	-2.80	2.85e-01; 1.59e-03	Soluble

### 3.6. Pharmacokinetics of ligands and FDA-approved drugs

The pharmacokinetics of the ligands (resveratrol, pterostilbene, oxyresveratrol, piceatannol, pinosylvin, isorhapontigenin, isorhapontin, astringin, piceid (polydatin), and mulberroside A) and FDA-approved drugs (tacrine, donepezil, rivastigmine, galantamine, and memantine) are shown in Table 5.

Pharmacokinetic properties of drugs, GI absorption, BBB permeant, P-gp substrate, CYP enzyme inhibitory (CYP1A2, CYP2C19, CYP2C9, CYP2D6, CYP3A4) and skin permeability coefficient. It is evaluated with various parameters such as (Log Kp). GI absorption determines the absorption of the drug from the intestines and its passage into the systemic circulation. P-gp substrates refer to drugs that are excreted from the cell by the active transport mechanisms of P-gp, which affects the bioavailability of drugs (Yoshitomo et al., 2022). Enzyme inhibitors such as CYP1A2, CYP2C19, CYP2C9, CYP2D6 and CYP3A4 may cause drug-drug interactions by inhibiting enzymes involved in drug metabolism. Inhibition of these enzymes can directly affect the metabolism and effectiveness of other drugs (Liao et al., 2020). Additionally, the skin permeability coefficient (Log Kp) determines the transdermal absorption capacity of drugs and their passage through the skin into the systemic circulation (Hamadeh et al., 2023). These parameters play an important role in drug development processes by providing critical information about the bioavailability, effectiveness and safety of drugs.

GI absorption, BBB permeant, P-gp substrate properties of ligands and FDA-approved drugs are also given in the BOILED-Egg plot. All ligands and FDA-approved drugs, except isorhapontin, astringin,

and mulberroside A, are within the optimum range for GI absorption. All ligands and FDA-approved drugs, except oxyresveratrol, piceatannol, isorhapontin, astringin, piceid (polydatin), and mulberroside A, are within the optimum range for BBB permeant. All ligands and FDA-approved drugs, except isorhapontin, piceid (polydatin), tacrine, donepezil, and galantamine, are not the substrate of P-gp.

The tendency of ligands and FDA-approved drugs to cause drug interactions through inhibition of cytochromes (CYPs) has been estimated (Hakkola et al., 2020). Ligands (isorhapontin, astringin, piceid (polydatin), and mulberroside A) and FDA-approved drugs (rivastigmine and memantine) are not the inhibitor of CYP1A2, CYP2C19, CYP2C9, CYP2D6, and CYP3A4.

Skin permeation is a linear method based on Potts and Guy's simple QSPR model, which relates the decimal logarithm of the skin permeability coefficient (log Kp in cm/s) to MW and log Po/w (Ranjith et al., 2022). Ligands and FDA-approved drugs with a lower negative log Kp value is seen as being more permeant to the skin (Jose et al., 2023). Log Kp (skin permeation) of ligands and FDA-approved drugs score ranges from -10.36 to -5.06 cm/s.

**Table 5.** Pharmacokinetics of ligands and FDA-approved drugs

No	Pharmacokinetic								
	GI absorption	BBB permeant	P-gp substrate	CYP1A2 inhibitor	CYP2C19 inhibitor	CYP2C9 inhibitor	CYP2D6 inhibitor	CYP3A4 inhibitor	Log Kp (skin permeation)
1	High	Yes	No	Yes	No	Yes	No	Yes	-5.47 cm/s
2	High	Yes	No	Yes	Yes	Yes	Yes	No	-5.18 cm/s
3	High	No	No	Yes	No	Yes	No	Yes	-5.82 cm/s
4	High	No	No	Yes	No	Yes	No	Yes	-5.76 cm/s
5	High	Yes	No	Yes	No	Yes	No	No	-5.12 cm/s
6	High	Yes	No	Yes	No	Yes	No	Yes	-5.33 cm/s
7	Low	No	Yes	No	No	No	No	No	-8.11 cm/s
8	Low	No	No	No	No	No	No	No	-8.26 cm/s
9	High	No	Yes	No	No	No	No	No	-7.95 cm/s
10	Low	No	No	No	No	No	No	No	-10.36 cm/s
11	High	Yes	Yes	Yes	No	No	No	Yes	-5.59 cm/s
12	High	Yes	Yes	No	No	No	Yes	Yes	-5.58 cm/s
13	High	Yes	No	No	No	No	No	No	-6.20 cm/s
14	High	Yes	Yes	No	No	No	Yes	No	-6.75 cm/s
15	High	Yes	No	No	No	No	No	No	-5.06 cm/s

### 3.7. Druglikeness of ligands and FDA-approved drugs

The druglikeness of the ligands (resveratrol, pterostilbene, oxyresveratrol, piceatannol, pinosylvin, isorhapontigenin, isorhapontin, astringin, piceid (polydatin), and mulberroside A) and FDA-approved drugs (tacrine, donepezil, rivastigmine, galantamine, and memantine) are shown in Table 6.

The druglikeness is evaluated using five distinct rule-based filters (Gupta et al., 2020). Major pharmaceutical corporations [Lipinski (Pfizer), Ghose (Amgen), Veber (GSK), Egan (Pharmacia), and Muegge (Bayer)] frequently conduct analyses that lead to these rule-based filters (Yadav and Mohite, 2020). Lipinski's rule is based on properties such as molecular weight (less than 500 Daltons), octanol/water partition coefficient ( $\log P \leq 5$ ), number of hydrogen bond acceptors ( $\leq 10$ ), and number of hydrogen bond donors ( $\leq 5$ ). Ghose, Veber, Egan and Muegge rules include additional parameters such as molecular weight, polar surface area (TPSA), number of rotatable bonds (Soares et al., 2023). Ligands (resveratrol, pterostilbene, oxyresveratrol, piceatannol, pinosylvin, and isorhapontigenin), and

FDA-approved drugs (donepezil, rivastigmine, and galantamine) are within acceptable range for Lipinsky, Ghose, Veber, Egan, and Muegge filters.

Also, the Abbot bioavailability score attempts to estimate the probability that ligands and FDA-approved drugs will have at least 10% oral bioavailability or measurable Caco-2 permeability in rats (Chai et al., 2022). This semiquantitative rule-based score based on total charge, TPSA, and Lipinski filter violation identifies four classes of ligands and FDA-approved drugs with probabilities of 11%, 17%, 56%, or 85% (Ozioko and Gaiya, 2023). These evaluations provide critical information to optimize the bioavailability and effectiveness of drugs. All ligands and FDA-approved drugs are within acceptable range for Abbot bioavailability score (17% and 56%).

**Table 6.** Druglikeness of ligands and FDA-approved drugs

Druglikeness						
No	Lipinski	Ghose	Veber	Egan	Muegge	Bioavailability score
1	Yes; 0 violation	Yes	Yes	Yes	Yes	0.55
2	Yes; 0 violation	Yes	Yes	Yes	Yes	0.55
3	Yes; 0 violation	Yes	Yes	Yes	Yes	0.55
4	Yes; 0 violation	Yes	Yes	Yes	Yes	0.55
5	Yes; 0 violation	Yes	Yes	Yes	Yes	0.55
6	Yes; 0 violation	Yes	Yes	Yes	Yes	0.55
7	Yes; 1 violation: NHorOH>5	Yes	No; 1 violation: TPSA>140	No; 1 violation: TPSA>131.6	No; 1 violation: H-don>5	0.55
8	Yes; 1 violation: NHorOH>5	Yes	No; 1 violation: TPSA>140	No; 1 violation: TPSA>131.6	No; 2 violations: TPSA>150, H-don>5	0.55
9	Yes; 1 violation: NHorOH>5	Yes	Yes	No; 1 violation: TPSA>131.6	No; 1 violation: H-don>5	0.55
10	No; 3 violations: MW>500, NorO>10, NHorOH>5	No; 4 violations: MW>480, WLOGP<-0.4, MR>130, #atoms>70	No; 1 violation: TPSA>140	No; 1 violation: TPSA>131.6	No; 3 violations: TPSA>150, H-acc>10, H-don>5	0.17
11	Yes; 0 violation	Yes	Yes	Yes	No; 1 violation: MW<200	0.55
12	Yes; 0 violation	Yes	Yes	Yes	Yes	0.55
13	Yes; 0 violation	Yes	Yes	Yes	Yes	0.55
14	Yes; 0 violation	Yes	Yes	Yes	Yes	0.55
15	Yes; 0 violation	Yes	Yes	Yes	No; 2 violations: MW<200, Heteroatoms<2	0.55

### 3.8. Medicinal chemistry of ligands and FDA-approved drugs

The medical chemistry of the ligands (resveratrol, pterostilbene, oxyresveratrol, piceatannol, pinosylvin, isorhapontigenin, isorhapontin, astringin, piceid (polydatin), and mulberroside A) and FDA-approved drugs (tacrine, donepezil, rivastigmine, galantamine, and memantine) are shown in Table 7.

The phrase "Pan-Assay INterference compounds" (PAINs) encompasses a broad range of ligands and FDA-approved drugs that impede biological screening assays through diverse methods of action (Boateng et al., 2024). PAINs can complicate drug discovery processes by causing false positive results

in biological screening campaigns. Ligands and FDA-approved drugs had no alert in PAINS filter except piceatannol and astringin.

Brenk is a filter to identify ligands and FDA-approved drugs that are chemically reactive, metabolically unstable, and at risk levels (Sardar, 2023). FDA-approved drugs (tacrine, donepezil, rivastigmine, and memantine) had no alert in Brenk filter.

Leadlikeness is a tactical guideline for selecting starting points for chemical optimization in order to enhance the possibility of developing "drug-like" molecules during the drug discovery programs (Goodnow, 2001). FDA-approved drugs (rivastigmine and galantamine) had no violation in leadlikeness.

The synthetic accessibility score of the ligands and FDA-approved drugs, or ease of synthesis, goes from 1 (very simple) to 10 (extremely difficult) (Ertl and Schuffenhauer, 2009). These scores are critical in determining the synthesizability of drug candidates and their potential in development. Synthetic accessibility of ligands and FDA-approved drugs score ranges from 1.98 to 6.11.

**Table 7.** Medicinal chemistry of ligands and FDA-approved drugs

Medical chemistry				
No	PAINS	Brenk	Leadlikeness	Synthetic accessibility
1	0 alert	1 alert: stilbene	No; 1 violation: MW<250	2.02
2	0 alert	1 alert: stilbene	No; 1 violation: XLOGP3>3.5	2.29
3	0 alert	1 alert: stilbene	No; 1 violation: MW<250	2.36
4	1 alert: catechol_A	2 alerts: catechol, stilbene	No; 1 violation: MW<250	2.09
5	0 alert	1 alert: stilbene	No; 1 violation: : MW>250	1.98
6	0 alert	1 alert: stilbene	No; 1 violation: XLOGP3>3.5	2.22
7	0 alert	1 alert: stilbene	No; 1 violation: : MW>350	4.98
8	1 alert: catechol_A	2 alerts: catechol, stilbene	No; 1 violation: MW>350	4.86
9	0 alert	1 alert: stilbene	No; 1 violation: MW>350	4.82
10	0 alert	1 alert: stilbene	No; 2 violations: MW>350, Rotors>7	6.11
11	0 alert	0 alert	No; 1 violation: MW<250	2.08
12	0 alert	0 alert	No; 2 violations: MW>350, XLOGP3>3.5	3.36
13	0 alert	0 alert	Yes	2.73
14	0 alert	1 alert: isolated_alkene	Yes	4.57
15	0 alert	0 alert	No; 1 violation: MW<250	3.70

### 3.9. Molecular docking results of ligands, FDA-approved drugs, and target proteins

The molecular docking results of the ligands (resveratrol, pterostilbene, oxyresveratrol, piceatannol, pinosylvin, isorhapontigenin, isorhapontin, astringin, piceid (polydatin), and mulberroside A), FDA-approved drugs (tacrine, donepezil, rivastigmine, galantamine, and memantine) and target proteins

(AChE, BuChE, APP, BACE, GSK-3 $\beta$ , CDK5, SOD, CAT, GPx, Cox-2, iNOS, IL-1 $\beta$ , and TNF- $\alpha$ ) are shown in Table 8.

Blind docking is a molecular modeling technique used to determine the binding sites of ligands to target proteins. This technique is used to predict the binding affinity and potential interactions of ligands. The vina score is a system based on empirical scoring that establishes the binding affinity of ligands, FDA-approved drugs, and target proteins (Boyles, 2020). Vina scores often indicate Gibbs free energy in the binding of ligands and FDA-approved drugs to target proteins (Akhoon et al., 2019). A higher negative vina score indicates a strong binding affinity (Meli et al., 2022). Such studies play a critical role in drug discovery and development processes and enable the development of more effective therapeutic strategies.

The binding affinity of the target proteins to ligands are AChE > CAT > Cox-2 > BuChE > iNOS > SOD > CDK5 > TNF- $\alpha$  > GPx > GSK-3 $\beta$  > APP > BACE > IL-1 $\beta$ , respectively. The binding affinity of the ligands to target proteins are mulberroside A > astringin > piceid (polydatin) > isorhapontin > oxyresveratrol > piceatannol > isorhapontigenin > resveratrol > pinosylvin > pterostilbene, respectively. The binding affinity of the target proteins to FDA-approved drugs are AChE > BuChE > Cox-2 > iNOS > CAT > SOD > GSK-3 $\beta$  > GPx > CDK5 > TNF- $\alpha$  > APP > BACE > IL-1 $\beta$ , respectively. The binding affinity of the FDA-approved drugs to target proteins are donepezil > galantamine > tacrine > rivastigmine > memantine, respectively. The molecular docking studies indicate that the ligands and FDA-approved drugs have a strong binding affinity to the target proteins (AChE, BuChE, APP, BACE, GSK-3 $\beta$ , CDK5, SOD, CAT, GPx, Cox-2, iNOS, IL-1 $\beta$ , and TNF- $\alpha$ ), and that it is possible for those proteins to function.

**Table 8.** Molecular docking results (vina score) of ligands, FDA-approved drugs, and target proteins

Ligand	Target Protein												
	AChE	BuChE	APP	BACE	GSK-3 $\beta$	CDK5	SOD	CAT	GPx	Cox-2	iNOS	IL-1 $\beta$	TNF- $\alpha$
Resveratrol	-8.7	-8.7	-7.2	-6.6	-6.9	-7.7	-8.1	-8.7	-7.1	-7.1	-8.6	-6.4	-7.7
Pterostilbene	-8.5	-8.0	-7.2	-6.7	-6.8	-7.1	-7.7	-8.3	-7.1	-7.9	-8.4	-6.1	-6.9
Oxyresveratrol	-8.8	-8.6	-7.5	-6.7	-7.3	-8.8	-8.2	-9.4	-7.0	-8.4	-8.6	-6.5	-7.5
Piceatannol	-9.1	-8.4	-7.1	-6.7	-7.0	-8.0	-8.5	-9.0	-7.1	-8.3	-9.0	-6.4	-7.9
Pinosylvin	-8.6	-8.4	-7.1	-6.3	-7.0	-7.6	-7.9	-8.3	-7.0	-7.9	-8.3	-6.0	-7.3
Isorhapontigenin	-8.8	-8.1	-7.0	-6.7	-7.0	-7.9	-7.8	-8.7	-7.3	-8.3	-8.2	-6.4	-7.9
Isorhapontin	-8.9	-9.1	-7.6	-8.1	-8.5	-9.2	-8.9	-9.3	-8.5	-10.5	-9.4	-7.3	-8.8
Astringin	-10.7	-9.4	-7.8	-8.1	-8.3	-8.9	-8.9	-9.9	-8.5	-10.6	<b>-10.0</b>	-7.2	-8.9
Piceid (polydatin)	-10.5	-9.8	-7.9	-7.8	-7.8	-8.9	-8.6	<b>-11.2</b>	-8.3	-10.1	-9.8	-7.4	-9.0
Mulberroside A	<b>-11.4</b>	<b>-10.2</b>	-8.5	<b>-8.8</b>	-8.7	-9.0	<b>-9.9</b>	-10.2	<b>-9.9</b>	<b>-10.8</b>	-9.2	<b>-7.8</b>	<b>-9.3</b>
Tacrine	-8.5	-8.2	-6.7	-6.5	<b>-9.9</b>	-8.1	-7.4	-8.0	-7.1	-8.1	-8.0	-5.6	-7.2
Donepezil	-10.0	-9.2	<b>-8.9</b>	-8.0	-7.6	<b>-9.7</b>	-7.9	-8.6	-9.0	-9.6	-9.3	-6.7	-8.4
Rivastigmine	-7.9	-7.1	-5.8	-5.7	-5.6	-6.1	-6.8	-7.5	-6.2	-6.8	-7.6	-5.3	-6.1
Galantamine	-8.7	-8.6	-7.0	-7.2	-7.5	-7.0	-8.1	-8.1	-7.9	-8.5	-8.1	-6.4	-7.8
Memantine	-7.6	-7.1	-5.8	-5.8	-6.6	-5.3	-7.5	-6.6	-6.4	-6.6	-6.3	-5.0	-6.5

In our study, the contact residues of the prominent ligands (astrin, piceid (polydatin), and mulberroside A) and FDA-approved drugs (tacrine and donepezil) to the target proteins (AChE, BuChE, APP, BACE, GSK-3 $\beta$ , CDK5, SOD, CAT, GPx, Cox-2, iNOS, IL-1 $\beta$ , and TNF- $\alpha$ ) according to their vina scores (kcal/mol) are given in Table 9.

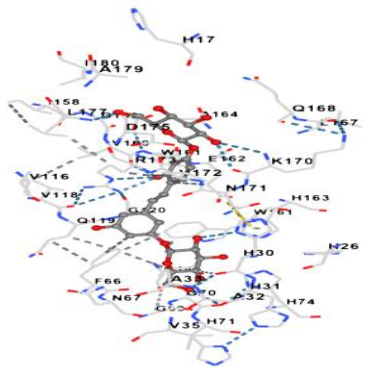
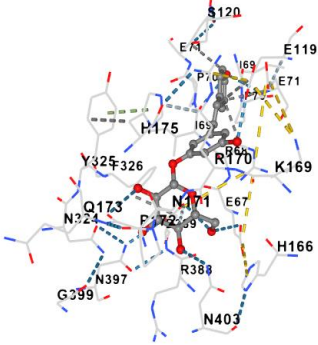
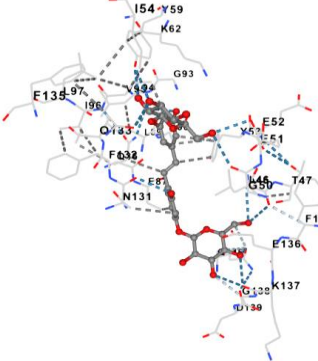
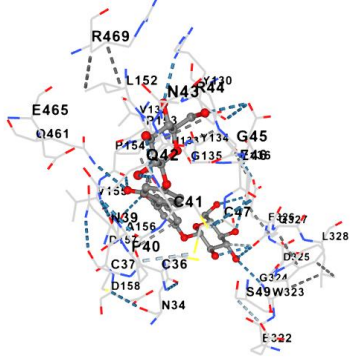
Interactions between ligands and target proteins are characterized by specific amino acid residues and bond structures at binding sites. These interactions are of great importance for the stability and function of biomolecular complexes. Various types of bonds, such as hydrogen bonds, hydrophobic interactions and electrostatic interactions, are the main components of these interactions. Interactions between hydrogen bonds are shown as teal dotted lines, and these bonds represent strong polar interactions between the ligand and the protein (Moharana et al., 2023). Hydrophobic interactions are shown with gray dotted connections, and these bonds represent interactions occurring in nonpolar regions between the ligand and the protein (Labarre et al., 2021). Electrostatic interactions are shown as yellow dotted lines, and these bonds express the attractive forces that occur between oppositely charged regions between the ligand and the protein (Fanfrlík et al., 2023). Detailed examination of these binding interactions is critical in drug discovery and development processes. Understanding the structural properties of ligand-protein complexes and the effects of these interactions on biological activity allows the design of new and more effective therapeutic agents (Adhav and Saikrishnan, 2023).

**Table 9.** Molecular docking results of ligands (astrin, piceid (polydatin), and mulberroside A) and FDA-approved drugs (tacrine and donepezil), and target proteins

Ligand	Target Protein	Contact Residues	
Mulberroside A	AChE	Chain B: GLN71 TYR72 ASP74 LEU76 THR83 TRP86 ASN87 TRP117 TYR119 GLY120 GLY121 GLY122 PHE123 TYR124 SER125 GLY126 ALA127 LEU130 TYR133 GLU202 SER203 ALA204 TRP236 TRP286 HIS287 VAL288 LEU289 PRO290 GLN291 GLU292 SER293 VAL294 PHE295 ARG296 PHE297 TYR337 PHE338 VAL340 TYR341 GLY342 HIS447 GLY448 ILE451	
Mulberroside A	BuChE	Chain A: GLN67 ASN68 ILE69 ASP70 GLN71 SER72 GLY78 SER79 TRP82 ASN83 PRO84 TYR114 GLY115 GLY116 GLY117 PHE118 GLN119 THR120 GLY121 THR122 LEU125 TYR128 GLY149 GLU197 SER198 LEU273 GLU276 ALA277 PHE278 VAL280 TYR282 GLY283 THR284 PRO285 LEU286 SER287 VAL288 ASN289 PHE290 ALA328 PHE329 VAL331 TYR332 GLY333 TRP430 MET437 HIS438 GLY439 TYR440 ILE442	

Donepezil	APP	<p>Chain A: ASN326 MET329            ARG330 ALA333            Chain B: ARG414 LEU417            ARG418 GLU420 GLN421            LYS422 GLN424 ARG425 HIS450            LEU453 GLN454 ILE456 GLU457            GLU458 VAL460 ASN461            LEU464 GLU483 LEU484            LEU485 HIS486 SER487</p>	
Mulberroside A	BACE	<p>Chain A: GLY11 GLN12 GLY13            LEU30 ASP32 GLY34 SER35            SER36 PHE47 TYR71 THR72            GLN73 GLY74 LYS107 PHE108            PHE109 ILE110 ASN111 SER113            TRP115 ILE118 ILE126 ARG128            TYR198 LYS224 ILE226 ASP228            SER229 GLY230 THR231            THR232 ASN233 ARG235            SER327 THR329 GLY330            THR331 VAL332</p>	
Tacrine	GSK-3β	<p>Chain A: ILE62 PHE67 VAL70            ALA83 LYS85 ARG96 GLU97            LEU132 TYR134 VAL135            THR138 ARG180 ASP181 LYS183            GLN185 ASN186 LEU188            CYS199 ASP200 PHE201 GLY202            SER203 ASN213 VAL214 SER215            TYR216 ILE217 ARG220 TYR221            GLY259 ASP260 SER261            Chain B: ARG220 TYR221            TYR222 PHE229 ASP260 VAL263            LEU266 VAL267 ILE270 PHE291            LYS292 PHE293 PRO294</p>	
Donepezil	CDK5	<p>Chain A: ARG149 PRO154            VAL155 ARG156 CYS157            TYR158 SER159 ALA160            GLU161 GLY175 ALA176            LYS177 PRO234 ASP235            Chain C: ARG179 ASP182            ARG183 LEU186 GLN191            ASP192 GLN193 GLY194 PHE195            ILE196 THR197 PRO198 ALA199            ASN200 MET237 GLY238            ASN239 GLU240 TYR243</p>	



Mulberroside A	SOD	<p>Chain A: HIS17 ILE18 HIS26  LYS29 HIS30 HIS31 ALA32  ALA33 VAL35 PRO62 ALA63  PHE66 ASN67 GLY69 GLY70  HIS71 HIS74 PHE77 VAL116  GLY117 VAL118 GLN119  GLY120 GLN143 ILE158 ASP159  VAL160 TRP161 GLU162 HIS163  ALA164 LEU167 GLN168  LYS170 ASN171 VAL172  ARG173 PRO174 ASP175 LEU177  LYS178 ALA179 ILE180</p> <p>Chain B: GLN21 ILE22 LEU25  HIS26 LYS29 HIS30 HIS31  ALA32 ALA33 VAL35 ASN37  ALA63 PHE66 ASN67 GLY69  GLY70 HIS71 HIS74 VAL116  GLY117 VAL118 GLN119  GLY120 GLN143 ASP159 TRP161  GLU162 HIS163 ALA164 LEU167  ASN171 VAL172 ARG173  PRO174</p>	
Piceid (polydatin)	CAT	<p>Chain A: GLU67 ARG68 ILE69  PRO70 GLU71 ARG72 VAL73  ALA76 ALA117 GLU119 SER120  HIS166 LYS169 ARG170 ASN171  PRO172 GLN173 HIS175 PHE326  GLU330</p> <p>Chain B: ASP389</p> <p>Chain C: GLU67 ARG68 ILE69  PRO70 GLU71 ALA117 GLU119  SER120 HIS166 LYS169 ARG170  ASN171 HIS175 LEU176 LYS177  ASN324 TYR325 PHE326  GLU330</p> <p>Chain D: ARG388 ASP389  ASN397 GLY399 ASN403</p>	
Mulberroside A	GPx	<p>Chain A: GLU52 ILE54 GLN58  TYR59 LYS62 ASN83 GLN86  GLU87 GLU88 LEU89 ALA90  PRO91 GLY93 LEU94 VAL95  ILE96 LEU97 ASN131 PHE132  GLN133 PHE135</p> <p>Chain B: GLU42 TYR43 GLY44  ALA45 LEU46 THR47 ASP49  GLY50 GLU51 GLU52 TYR53  ILE54 PRO55 PHE99 PHE135  GLU136 LYS137 GLY138 ASP139  LYS144 GLU145 GLN146  LYS147 PHE148</p>	
Mulberroside A	Cox-2	<p>Chain C: ASN34 PRO35 CYS36  CYS37 SER38 ASN39 PRO40  CYS41 GLN42 ASN43 ARG44  GLY45 GLU46 CYS47 MET48  SER49 TYR130 ASN131 VAL132  HIS133 TYR134 GLY135 TYR136  TYR147 ALA151 LEU152  PRO153 PRO154 VAL155  ALA156 ASP157 ASP158 GLN461  GLU465 TYR466 LYS468  ARG469</p> <p>Chain D: GLU322 TRP323  GLY324 ASP325 GLU326  GLN327 LEU328</p>	

Astringin	iNOS	<p>Chain A: GLY117 SER118 ILE119 MET120 ARG199 CYS200 ILE201 GLY202 GLN263 ARG266 TRP346 TYR347 PRO350 VAL352 TYR373 MET374 THR376 GLU377 ILE378 ARG381 ASP382 ASP385 ARG388 ILE462 TRP463 LEU464 VAL465 PRO466 PRO467 PHE476</p> <p>Chain B: LYS88 TRP90 ALA197 PRO198 ARG199 CYS200 ILE201 GLY202 MET374 GLU377 ARG381 TRP461 ILE462 TRP463 LEU464 VAL465 PRO466 PRO467 VAL475 PHE476 HIS477 GLN478 GLU479 MET480</p>	
Mulberroside A	IL-1 $\beta$	<p>Chain A: GLY22 PRO23 TYR24 GLU25 LEU26 LYS74 LYS77 PRO78 THR79 LEU80 GLN81 LEU82 GLU83 SER84 TRP120 SER123 THR124 SER125 GLN126 ALA127 MET130 PRO131 VAL132 PHE133 LEU134 GLY135 GLY136 THR137 LYS138 GLN141 ASP142 ILE143</p>	
Mulberroside A	TNF- $\alpha$	<p>Chain B: GLU53 GLY54 LEU55 ARG82 ALA84 TYR87 LYS90 VAL91 ASN92 LEU93 LEU94 SER95 VAL123 PHE124 GLN125 LEU126 GLU127 LEU157</p> <p>Chain D: ARG82 ILE83 ALA84 TYR87 GLN88 THR89 VAL91 ASN92 LEU93 LEU94 SER95 ALA96 ILE97 LYS98 TYR119 LEU120 GLY121 VAL123 PHE124 GLN125 LEU126 GLU127</p>	

#### 4. Conclusions

In conclusion, comprehensive evaluation of stilbenes and FDA-approved drugs through computational methodologies targeting many hypotheses underlying AD pathogenesis has provided valuable insights into their potential therapeutic efficacy. Further investigation and validation of these findings through *in vitro* and *in vivo* studies are warranted to translate these computational predictions into clinically meaningful treatments for AD.

#### Statement of Conflict of Interest

The author of the article declares that she has no conflict of interest.

## Author's Contributions

The author declares that she has contributed 100% to the article.

## References

- Akhood BA., Tiwari H., Nargotra A. In silico drug design methods for drug repurposing. In: *In Silico Drug Design*. Cambridge, Academic Press 2019; 47-84.
- Aleynova OA., Ogneva ZV., Suprun AR., Ananov AA., Nityagovsky NN., Beresh AA., Dubrovina AS., Kiselev KV. The effect of external treatment of *Arabidopsis thaliana* with plant-derived stilbene compounds on plant resistance to abiotic stresses. *Plants* 2024; 13(2): 184.
- Balakrishnan R., Jannat K., Choi DK. Development of dietary small molecules as multi-targeting treatment strategies for Alzheimer's disease. *Redox Biol.* 2024; 103105.
- Boateng ST., Roy T., Agbo ME., Mahmud MA., Banang-Mbeumi S., Chamcheu RCN., Yadav RK., Pham LK., Dang DD., Jackson KE, Nagalo BM, Efimova T., Fotie J., Chamcheu JC. Multifaceted approach toward mapping out the anticancer properties of small molecules via in vitro evaluation on melanoma and nonmelanoma skin cancer cells, and in silico target fishing. *Chem. Biol. Drug Des.* 2024; 103(1).
- Boobier S., Hose DRJ., Blacker A., Nguyen B. Machine learning with physicochemical relationships: solubility prediction in organic solvents and water. *Nature Communications* 2020; 11: 521.
- Boyles F. Developing novel scoring functions for protein-ligand docking using machine learning. Doctoral Dissertation, University of Oxford 2020.
- Buchwald P., Bodor N. Octanol-water partition: Searching for predictive models. *Curr. Med. Chem.* 1998; 5(5): 353-380.
- Cao W., Zheng B., Zeng X., He H., Chen L. Stilbene, as phyto-oestrogens, can construct resistant starch through noncovalent interactions with starch: A structural correlation study. *Food Hydrocoll.* 2024; 148: 109438.
- Chai TT., Wong CCC., Sabri MZ., Wong FC. Seafood paramyosins as sources of anti-angiotensin-converting-enzyme and anti-dipeptidyl-peptidase peptides after gastrointestinal digestion: A cheminformatic investigation. *Molecules* 2022; 27(12): 3864.
- Ciorsac A., Filip M., Isvoran A. Predict of water solubility of the low molecular weigh oligomers of polyhydroxyalkanoates. *New Front. Chem.* 2021; 30(1): 25-34.
- Daina A., Michielin O., Zoete V. SwissADME: a free web tool to evaluate pharmacokinetics, drug-likeness and medicinal chemistry friendliness of small molecules. *Scientific Rep.* 2017; 7(1): 42717.
- Daina A., Zoete V. A boiled-egg to predict gastrointestinal absorption and brain penetration of small molecules. *ChemMedChem* 2016; 11(11): 1117-1121.
- Ertl P., Schuffenhauer A. Estimation of synthetic accessibility score of drug-like molecules based on molecular complexity and fragment contributions. *J. Cheminform.* 2009; 1: 1-11.

- Ganz T., Ben-Hur T. The “hit and run” hypothesis for Alzheimer’s disease pathogenesis. *Int. J. Mol. Sci.* 2024; 25(6): 3245.
- Goodnow Jr RA. Current practices in generation of small molecule new leads. *J. Cell. Biochem.* 2001; 84(S37): 13-21.
- Gupta PP., Bastikar VA., Bastikar A., Chhajed SS., Pathade PA. Computational screening techniques for Lead design and development. *CADD* 2020; 187-222.
- Hakkola J., Hukkanen J., Turpeinen M., Pelkonen O. Inhibition and induction of CYP enzymes in humans: an update. *Arch. Toxicol.* 2020; 94(11): 3671-3722.
- Henning N., Kannigadu C., Aucamp J., van Rensburg HDJ., David DD. Probing benzothiadiazine-1, 1-dioxide ethylene glycol derivatives against Leishmania: synthesis and in vitro efficacy evaluation. *Res Sq.* 2023; PPR664243.
- Ibrahim MT., Uzairu A., Uba S., Shallangwa GA. Computational modeling of novel quinazoline derivatives as potent epidermal growth factor receptor inhibitors. *Heliyon* 2020; 6(2).
- Jia CY., Li JY., Hao GF., Yang GF. A drug-likeness toolbox facilitates ADMET study in drug discovery. *Drug Discov. Today* 2020; 25(1): 248-258.
- Jose S., Devi SS., Sajeev A., Girisa S., Alqahtani MS., Abbas M., et al. Repurposing FDA-approved drugs as FXR agonists: a structure based in silico pharmacological study. *Biosci. Rep.* 2023; 43(3).
- Kadri A., Aouadi K. In vitro antimicrobial and  $\alpha$ -glucosidase inhibitory potential of enantiopure cycloalkylglycine derivatives: Insights into their in silico pharmacokinetic, druglikeness, and medicinal chemistry properties. *Journal of Applied Pharmaceutical Science* 2020; 10(6): 107-115.
- Kamble SM., Patil KR., Upaganlawar AB. Etiology, pathogenesis of Alzheimer's disease and amyloid beta hypothesis. In: *Alzheimer's Disease and Advanced Drug Delivery Strategies*. Cambridge, Academic Press 2024; 1-11.
- Liao M., Jaw-Tsai S., Beltman J., Simmons A., Harding T., Xiao JJ. Evaluation of in vitro absorption, distribution, metabolism, and excretion and assessment of drug-drug interaction of rucaparib, an orally potent poly(ADP-ribose) polymerase inhibitor. *Xenobiotica* 2020; 50: 1032-1042.
- Liu N., Liang X., Chen Y., Xie L. Recent trends in treatment strategies for Alzheimer's disease and the challenges: A topical advancement. *Ageing Res. Rev.* 2024; 102199.
- Liu Y., Yang X., Gan J., Chen S., Xiao ZX., Cao Y. CB-Dock2: Improved protein–ligand blind docking by integrating cavity detection, docking and homologous template fitting. *Nucleic Acids Res.* 2022; 50(W1).
- Meli R., Morris GM., Biggin PC. Scoring functions for protein-ligand binding affinity prediction using structure-based deep learning: A review. *Front. Bioinform.* 2022; 2: 885983.
- Mishra S., Dahima R. In vitro ADME studies of TUG-891, a GPR-120 inhibitor using SWISS ADME predictor. *JDDT* 2019; 9(2-s): 366-369.

- Moharana M., Pattanayak SK., Khan F. Molecular recognition of bio-active triterpenoids from *Swertia chirayita* towards hepatitis Delta antigen: a mechanism through docking, dynamics simulation, Gibbs free energy landscape. *J. Biomol. Struct. Dyn.* 2023; 41(24).
- Nasb M., Tao W., Chen N. Alzheimer's disease puzzle: Delving into pathogenesis hypotheses. *Aging Dis.* 2024; 15(1): 43-73.
- Ndombera F., Maiyoh G., Tuei V. Pharmacokinetic, physicochemical and medicinal properties of n-glycoside anti-cancer agent more potent than 2-deoxy-d-glucose in lung cancer cells. *J. Pharm. Pharmacol.* 2019; 7(4): 165-176.
- Ozioko PC., Gaiya DD., Abdullahi I. Essential secondary metabolites of *Azadirachta indica* leaf in search of drug for COVID-19 treatment: In-silico ADMET and bioactivity predictions. *Int. J. Adv. Res. Biol. Sci.* 2023; 10(9): 79-93.
- Perluigi M., Di Domenico F., Butterfield DA. Oxidative damage in neurodegeneration: Roles in the pathogenesis and progression of Alzheimer disease. *Physiol. Rev.* 2024; 104(1): 103-197.
- Poltronieri P., Xu B., & Giovinzano G. Resveratrol and other stilbenes: effects on dysregulated gene expression in cancers and novel delivery systems. *Anti-Cancer Agents in Medicinal Chemistry* 2020.
- Ponzoni I., Sebastián-Pérez V., Requena-Triguero C., Roca C., Martínez MJ., Cravero F., Diaz MF., Paez JA., Arrayas RG., Adrio J., Campillo NE. Hybridizing feature selection and feature learning approaches in QSAR modeling for drug discovery. *Sci. Rep.* 2017; 7(1): 2403.
- Rafeeq MM., Helmi N., Sain ZM., Iqbal J., Alzahrani A., Alkurbi MO., Shater AF., Al-ahmadi BM., Alam MZ., Alam Q. Target-based virtual screening and molecular dynamics approach to identify potential antileishmanial agents through targeting UvrD-like helicase ATP-binding domain. *Adv. Life Sci* 2024; 11(1): 237-245.
- Ranjith D., Padhi PK., Dhaval JK., Karikalan M., Naveena M., Johnson BE., Telang AG. Insilco prediction and hematological alterations in male rats exposed to Ethion and its amelioration by nano-quercetin: A sub chronic study. *J. Pharm. Innov.* 2022; 11(11): 1116-1122.
- Ranjith D., Ravikumar C. SwissADME predictions of pharmacokinetics and drug-likeness properties of small molecules present in *Ipomoea mauritiana* Jacq. *J Pharmacogn Phytochem* 2019; 8(5): 2063-2073.
- Sardar H. Drug like potential of Daidzein using SwissADME prediction: In silico Approaches. *PHYTONutrients* 2023; 02-08.
- Sert M., Işıl Ö., Yaglioglu AS., Bulut A. Gabriel-Cromwell aziridination of amino sugars; chiral ferrocenoyl-aziridiny sugar synthesis and their biological evaluation. *Carbohydr. Res.* 2021; 509: 108430.
- Shevelyova MP., Deryusheva EI., Nemashkalova EL., Machulin AV., Litus EA. Role of human serum albumin in the prevention and treatment of Alzheimer's disease. *Biol. Bull. Rev.* 2024; 14(1): 29-42.

- Soares A., Sousa G., Calil R., & Trossini G. Absorption matters: A closer look at popular oral bioavailability rules for drug approvals. *Molecular Informatics* 2023; 42.
- Socala K., Żmudzka E., Lustyk K., Zagaja M., Brighenti V., Costa AM., Andres-Mach M., Pytka K., Martinelli I., Mandrioli J., Pellati F., Biagini G., Wlaz P. Therapeutic potential of stilbenes in neuropsychiatric and neurological disorders: A comprehensive review of preclinical and clinical evidence. *Phytother. Res.* 2024; 38(3): 1400-1461.
- Udugade SB., Dojjad RC., Udugade BV. In silico evaluation of pharmacokinetics, drug-likeness and medicinal chemistry friendliness of momordicin1: An active chemical constituent of momordica charantia. *J. Adv. Sci. Res.* 2019; 10(03 Suppl 1): 222-229.
- Vejanndla B., Savani S., Appalaneni R., Veeravalli RS., Gude SS. Alzheimer's disease: The past, present, and future of a globally progressive disease. *Cureus* 2024; 16(1).
- Wolfe MS.  $\gamma$ -Secretase: once and future drug target for Alzheimer's disease. *Expert Opin. Drug Discov.* 2024; 19(1): 5-8.
- Yadav AR., Mohite SK. ADME analysis of phytochemical constituents of Psidium guajava. *Asian J. Sci. Res.* 2020; 13(5): 373-375.
- Yağlıoğlu AŞ., Gürbüz DG., Dölarslan M., Demirtaş İ. First determination of anticancer, cytotoxic, and in silico ADME evaluation of secondary metabolites of endemic *Astragalus leucothrix* Freyn & Bornm. *Turk. J. Chem.* 2022; 46(1); 169-183.
- Yajing M., Sufang L., Qingfeng Z., Zhonghua L., Zhijian Z., Bin Y. Approved drugs and natural products at clinical stages for treating Alzheimer's disease. *Chin J Nat Med* 2024; 22(0): 1-12.
- Yan QW., Su BJ., He S., Liao HB., Wang HS., Liang D. Structurally diverse stilbenes from *Gnetum parvifolium* and their anti-neuroinflammatory activities. *Bioorg. Chem.* 2024; 143: 107060.
- Yoshitomo A., Asano S., Hozuki S., Tamemoto Y., Shibata Y., Hashimoto N., Takahashi K., Sasaki Y., Ozawa N., Kageyama M., Iijima T., Kazuki Y., Sato H. Significance of basal membrane permeability of epithelial cells in predicting intestinal drug absorption. *Drug Metabolism and Disposition* 2022; 51: 318-328.